Wireless Design of a Multisensor System for Physical Activity Monitoring

Lingfei Mo, *Member, IEEE*, Shaopeng Liu, *Student Member, IEEE*, Robert X. Gao*, *Fellow, IEEE*, Dinesh John, John W. Staudenmayer, and Patty S. Freedson

***Abstract*—Real-time monitoring of human physical activity (PA) is important for assessing the intensity of activity and exposure to environmental pollutions. A wireless wearable multisenor integrated measurement system (WIMS) has been designed for real-time measurement of the energy expenditure and breathing volume of human subjects under free-living conditions. To address challenges posted by the limited battery life and data synchronization requirement among multiple sensors in the system, the ZigBee communication platform has been explored for energy-efficient design. Two algorithms have been developed (multiData packaging and slot-data-synchronization) and coded into a microcontroller (MCU)-based sensor circuitry for real-time control of wireless data communication. Experiments have shown that the design enables continued operation of the wearable system for up to 68 h, with the maximum error for data synchronization among the various sensor nodes (SNs) being less than 24 ms. Experiment under free-living conditions have shown that the WIMS is able to correctly recognize the activity intensity level 86% of the time. The results demonstrate the effectiveness of the energy-efficient wireless design for human PA monitoring.**

***Index Terms*—Data synchronization, energy efficiency, physical activity (PA) monitoring, wireless sensor networks.**

I. Introduction

PHYSICAL activity (PA) increases the fitness level and exercise capacity, helps reduce risk factors such as obesity, diabetes, blood pressure, and lipid abnormalities, improves health of the cardiovascular system, and extends life expectancy [1]. Real-time monitoring of PA of human subjects and their exposure to environmental pollutions provide an objective means for assessing the energy expenditure of the subjects, thus is of significant interest to the healthcare and medical communities. Traditionally, energy expenditure and environmental exposure of human are determined from the oxygen consumption and carbon dioxide release, measured by a mouthpiece [2]. Such a technique is not practical for applications in free-living environments. In recent years, PA monitoring through accelerometers has seen rapid increase. This technique offers noninvasive and low-cost measurement with low subject burden [3], [4], and studies [5] have shown effectiveness in using accelerometers for identifying PA intensities. However, using accelerometers alone has shown to be insufficient for distinguishing different types of activities. Furthermore, it does not quantify the human subject's exposure to environmental pollutions. To enable comprehensive and accurate assessment of PA intensity, type, energy expenditure and environmental exposure, multiple sensors are needed.

Recent advancement in wireless technology has enabled increasing applications of wireless sensors for monitoring physical activities and human health [6]–[8]. Compared to wired systems, wireless sensors eliminate interference with activities caused by wire tangling, thus are more convenient to wear [7], [9]. Accordingly, wireless body sensor or area networks have quickly grown into a promising technology for human health monitoring [10]–[14]. With the development of wireless implantable biosensors, the resulting sensor networks have been utilized for applications ranging from *in vivo* monitoring and intervention to everyday healthcare [7].

Two well-documented and tested wireless protocols—Bluetooth and ZigBee, have been widely used for wireless body area networks (WBANs) [15], [16]. Bluetooth has been conveniently used together with the mobile phone system [17]. Compared with Bluetooth, ZigBee features lower power consumption, lower cost, and lower data rate, with shorter "sleep" and "wake-up" times. It utilizes the carrier sense multiple access with collision avoidance (CSMA/CA) method to avoid data collision and improve the reliability in data communication [18]. Since the ZigBee and Bluetooth protocols are designed for wireless networks with a large number of sensors and longer data transmission range than typically seen in WBANs [15], it is necessary to modify the protocol in the hardware and software design of WBANs for optimized energy consumption [19] and improved reliability in real-time PA monitoring.

Several commercial wireless systems are available for PA monitoring. However, those systems are limited in various aspects, in terms of the ability to measure multiple parameters

Manuscript received February 15, 2012; revised May 2, 2012; accepted June 25, 2012. Date of publication July 12, 2012; date of current version October 16, 2012. This work was supported by the National Institutes of Health under Grant UO1 CA130783. *Asterisk indicates corresponding author.*

L. Mo is with the Electromechanical Systems Laboratory, Department of Mechanical Engineering, University of Connecticut, Storrs, CT 06269 USA, and also with the State Key Lab of Industrial Control Technology, Department of Control Science and Engineering, Zhejiang University, Hangzhou 310027, China (e-mail: lfmo@engr.uconn.edu).

S. Liu is with Electromechanical Systems Laboratory, Department of Mechanical Engineering, University of Connecticut, Storrs, CT 06269 USA (e-mail: sliu@engr.uconn.edu).

*R. X. Gao is with the Electromechanical Systems Laboratory, Department of Mechanical Engineering, University of Connecticut, Storrs, CT 06269 USA (e-mail: rgao@engr.uconn.edu).

D. John and P. S. Freedson are with the Physical Activity and Health Laboratory, Department of Kinesiology, University of Massachusetts, Amherst, MA 01003 USA (e-mail: djohn1@kin.umass.edu; psk@kin.umass.edu).

J. W. Staudenmayer is with the Department of Mathematics and Statistics, University of Massachusetts, Amherst, MA 01003 USA (e-mail: jstauden@math.umass.edu).

Color versions of one or more of the figures in this paper are available online at http://ieeexplore.ieee.org.

Digital Object Identifier 10.1109/TBME.2012.2208458

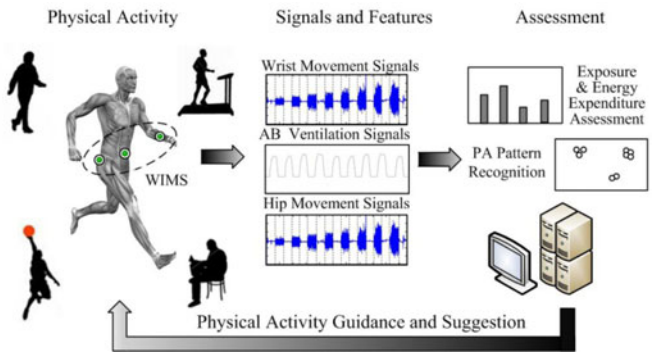

Fig. 1. WIMS for PA monitoring and assessment.

with high accuracy under free-living conditions, data synchronization among the various types of data measured, monitoring of ventilation/breathing, battery life, etc.

Motivated by the increasing demand for advanced PA monitoring and assessment techniques in free-living environments and with minimal subject burden, a ZigBee-based wireless wearable multisensor integrated measurement system (WIMS) has been designed, analyzed, prototyped, and experimentally evaluated. A major focus of the design is energy efficiency, as the capacity of the battery for powering the wireless sensor node (SN) is limited, whereas the expected operating time of the SN is not less than 20 h, to ensure reliable functioning of the circuit for daily testing. In addition to energy efficiency, data synchronization of multiple sensors contained in the WIMS is critical, as it provides the basis for establishing correlation among the various sensing data for PA pattern recognition and calculation of the metabolic equivalent of task (MET) [20]. However, given that data from various sensors are packaged together and transmitted periodically to the data logger, synchronization of multiple sensor data is not feasible as in the case of a wired multisensor measurement system. Furthermore, because of the inherent difference in clock accuracy among different SNs, data asynchronization may increase with time. In this study, an embedded protocol integrating two algorithms: multidata packaging and slot-data-dynchronization, have been designed for data synchronization and optimized energy efficiency. The protocol is specifically designed for wireless multisensor systems that monitor PAs in real time, under free-living conditions.

The rest of this paper is organized as follows: in Section II, the hardware design of the system is briefly introduced, whereas in Section III, the design of the wireless communication protocol is described in detail. Experimental results and discussions are provided in Section IV, and conclusions are drawn in Section V.

II. Hardware Design

A. System Configuration

The WIMS is designed to acquire data from human subjects engaged in PAs in real time, and extract characteristic parameters for PA assessment. For clinical acceptance, the design is required to 1) present a low subject burden, 2) have a continued operational life of $>$20 h, and 3) be easy to use. Fig. 1 illustrates the configuration of the WIMS.

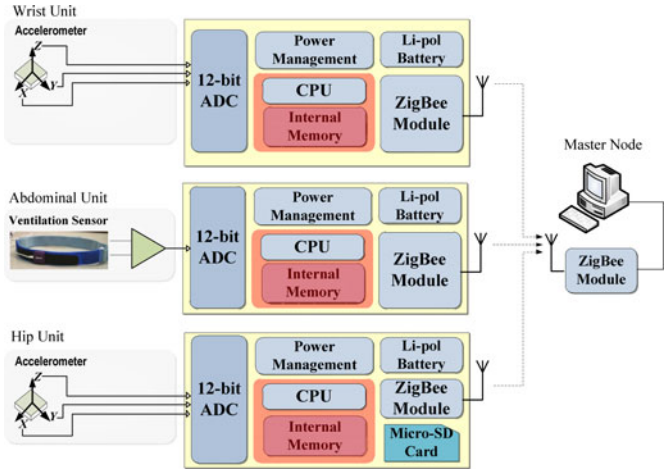

Fig. 2. Functional units and communication scheme of WMIS

The WIMS collects data on body motion and breathing from the human subject. The data are subsequently extracted and fused to quantify the energy expenditure and determine the PA types through an embedded pattern recognition algorithm. Three sensors of two different types are included in the WIMS.

1) Two triaxial accelerometers, worn at the hip and wrist, to measure the body and arm motions that characterize the degree of PA.
2) One displacement sensor, wrapped around the abdomen area, for measuring the expansion and contraction resulting from the ventilation (breathing rate and volume).

B. WIMS Realization

Fig. 2 illustrates the three functional units of the system—abdominal (AB) unit, wrist unit, and hip unit, with the related architectural diagram and wireless communication scheme. Each unit includes an 8-bit microcontroller (MCU) and a ZigBee module, enabling signal acquisition on-board and wireless data communication among the units. The AB Unit includes a piezoelectric displacement sensor for measuring respiration characteristics, i.e., breathing rate and volume. The wrist unit contains a triaxial accelerometer to measure the arm/upper body motions, and the hip unit contains another triaxial accelerometer for measuring body chunk motions. To preserve the fidelity of PA sensor, 30 Hz is chosen as the sampling rate for all these sensors [21]. The three units are designed with two modes of operations/network topologies: 1) signals measured by the AB unit and wrist unit are continuously transmitted to the hip unit through ZigBee, and all the data are stored into a 2-GB microsecure digital card located in the hip unit; 2) data from the three sensing units are wirelessly transmitted to a nearby master node (MN), such as a smartphone or computer. This mode of operation is the focus of the presented work.

C. Hardware Prototyping

The hardware design of the three functional units is prototyped as shown in Fig. 3 (with both front and back sides). Each unit consists of an MCU (MC9S08QE128, Freescale) and

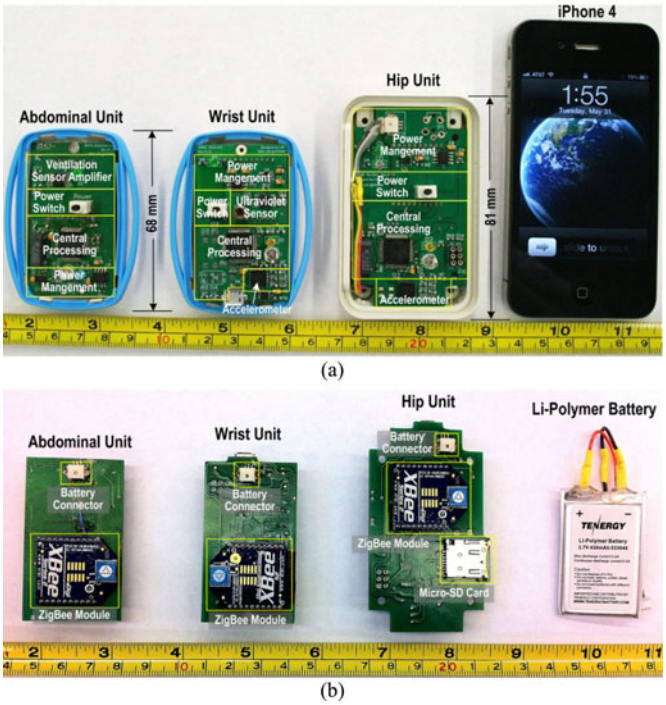

Fig. 3. Prototyping of WIMS functional units: (a) front side and (b) back side.

ZigBee Module (XBee-PRO, Digi International, Inc.). The MCU contains a 12-bit analog-to-digital converter (ADC) on-chip for digitizing analog sensor input. The ZigBee modules operate in the ISM frequency band of 2.4 GHz, and support low-power communication. The ZigBee module is located on the back of each circuit board, and transmits data to the computer through an XBee Explorer Dongle (WRL-09819, SparkFun Electronics, Inc.), which is connected via the USB-port to the computer. The band rate of the ZigBee module is 38 400 bit/s; accordingly, the maximal bandwidth of the sensor system is 38.4 kHz. This bandwidth satisfies the required maximal data recording rate of 7 sensors $\times$ 2 byte/sensor $\times$ 8 bit/byte $\times$ 30 Hz $=$ 3.36 kHz. In addition to the MCU and ZigBee module, each unit accommodates a 3.7 V Li-polymer battery and associated charging circuitry via a micro-USB connecter. Each PCB circuit board is prototyped as a double-layered board, containing IC components on both sides. The package size of the largest (hip) unit measures 81 mm $\times$ 53 mm $\times$ 14 mm ($L \times W \times H$), smaller than that of an iPhone.

III. Wireless Communication Protocol

A. WIMS Network Topology

The WIMS, as shown in Fig. 4, is built on a two-tiered network topology. In the lower tier, each of the SNs transmits data through ZigBee to an adjacent MN (such as a desktop computer, a laptop computer, or a smartphone). The MN in the upper tier then transmits data collected as packet to a monitoring station (MS) through WiFi or 3G, enabling data archival for PA assessment.

Each SN can operate in two modes: *passive* and *active*. In the *passive* mode, the SN transmits data whenever it receives a command from the MN. Accordingly, the SN is "ON" all the time, listening to the command from the MN. In the *active* mode, the SN transmits data to the MN at predetermined intervals only, and remains sleep during the nontransmitting period. The MN is kept in the receiving mode to ensure timely receipt of data from the SNs without data loss.

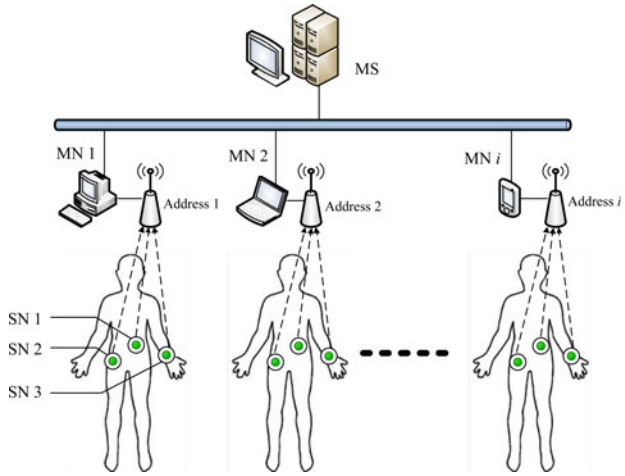

Fig. 4. WIMS network topology (MS $=$ monitoring station, MN $=$ master node, and SN $=$ sensor node).

Because of the limited capacity of batteries, energy efficiency has been one of the main constraints in wireless systems [15]. Given that the SNs sample and transmit data frequently when the human subject is engaged in physical activities, method to improve energy efficiency is needed for maximizing the battery life of the SNs.

When the SNs are in the active transmission mode, data collision and loss may occur [22], as each SN continuously samples and transmits data. Traditionally, data are transmitted immediately after they are sampled. This leads to high possibility of data collision, which is energy consuming, especially when the number of SNs increases. A communication protocol with anti-collision capability is needed to ensure data integrity and reduce energy consumption resulting from the need for repeated data transmission.

For accurate assessment of PA, data sampled from different SNs need to be synchronized after being received by the MN. Realistically, sensor data may be out of sync due to variation in the clock frequencies of different SNs. In addition, if data sampled in multiple consecutive cycles are packetized as one data frame and then transmitted, they can be asynchronous at the beginning of the communication as the start time of the data packaging could be different for different SNs. This problem becomes more significant as the packet size increases. Therefore, a protocol that assures data synchronization among the different SNs is needed [10].

B. Communication Protocol

The WIMS communication protocol is built on top of the ZigBee (IEEE 802.15.4) protocol and reconfigured with specific control strategies to realize low energy consumption and high communication performance.

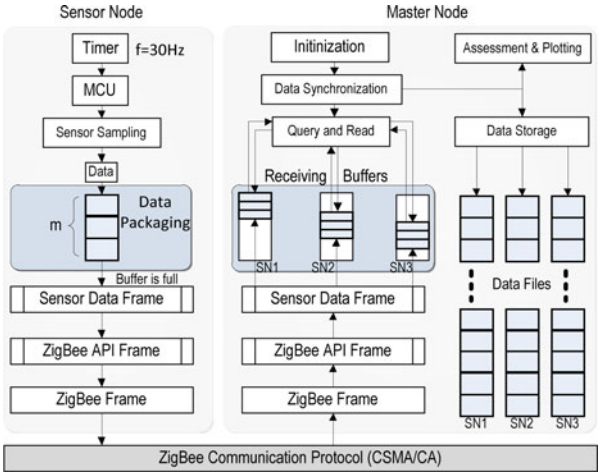

Fig. 5. Block diagram of the WIMS communication protocol.

Fig. 5 depicts the block diagram and flow control of the WIMS communication protocol for both the SN and MN. The MCU in the SN is woke up from the sleep mode by a timer interrupt every 33.3 ms, leading to a sampling rate of 30 Hz. The MCU samples sensor signals through an onboard 12-bit ADC, and stores the sampled data in a buffer before transmission. The size of the buffer is determined concurrently from a tradeoff analysis between energy efficiency and transmission latency, as described in the next section.

When the buffer is full, sensor data are packetized as one sensor data frame. This is subsequently packaged into an application program interface (API) data frame, and loaded into the ZigBee module for transmission. Each sensor data frame contains two bytes of sensor identification (ID), which is used for separating data frames received on the MN's end. Once the ZigBee is ready for transmission, the ZigBee API frame is parsed and repackaged into a ZigBee data frame which is then transmitted to the MN through the ZigBee protocol integrated within the CSMA/CA algorithm [18]. Once a ZigBee frame is received by the MN, it is first depacketized to obtain the sensor data and ID. The MN contains dedicated receiving buffers for each SN, and sensor data are temporarily allocated into the corresponding receiving buffer according to the sensor ID. The MN then queries and reads the receiving buffers continuously, and data of different SNs are synchronized through an embedded slot-data-synchronization algorithm. Subsequently, data are plotted and stored for PA assessment. In Fig. 6, the data frame structure is shown. Multiple sensor data are packetized into a sensor data frame and transferred to a ZigBee frame through a ZigBee API frame. The ZigBee communication protocol can be reconfigured in the ZigBee API frame.

1) Energy efficiency. In the WIMS communication protocol, energy efficiency is achieved by a multidata-packaging method. The SNs are configured to work in the *active* mode, and are powered up only during data transmission. For the rest of the time, the SNs are sleeping without idle listening. In addition, multiple sampling data stored in the SNs buffer are packetized into one packet for reduced energy consumption in data transmission. The energy consumption of the SN is quantified by its

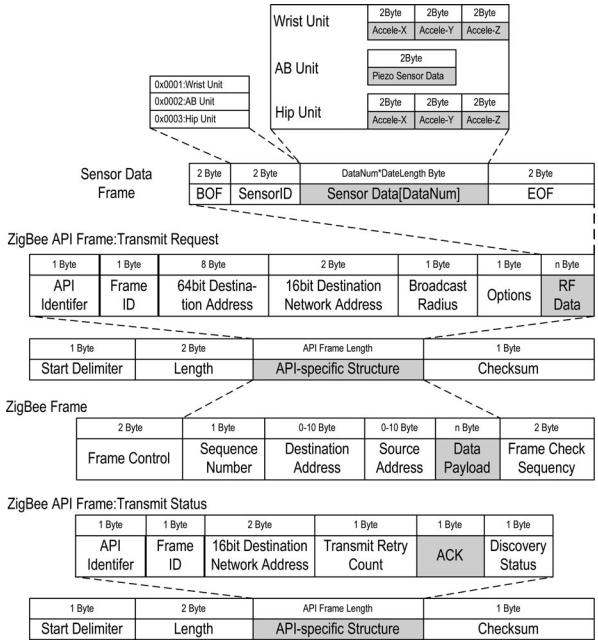

Fig. 6. Data frame structure.

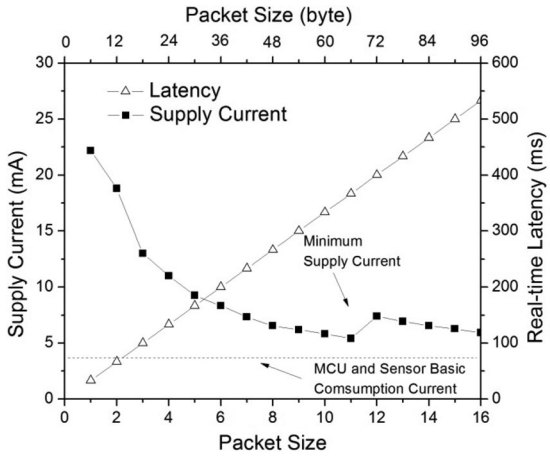

Fig. 7. Energy consumption and real-time latency for different data packet sizes. The square dots correspond to supply current, whereas the triangular dots correspond to latency (for wrist unit and hip unit).

supply current I_C, which is derived as

$$I_C = \frac{f_0}{m}\left(\frac{I_{sl}m}{f_0} - I_{sl}\Delta t_{\rm idle} - I_{sl}\Delta t_{\rm tr} + I_{\rm idle}\Delta t_{\rm idle} + I_{\rm tr}\Delta t_{\rm tr}\right) \quad (1)$$

where I_{sl} is the current consumed when the SN is sleeping, $I_{\rm idle}$ is the SNs idle current, $I_{\rm tr}$ is the data transmitting current, $\Delta t_{\rm idle}$ is the idle time, $\Delta t_{\rm tr}$ is the transmission time, f_0 is the sampling frequency, and m is the packet size. It is seen from (1) that the energy consumption will decrease if the packet size m increases. Such a decreasing trend between the current and packet size is demonstrated by experiments as shown in Fig. 7, where the square dots represent measured supply currents of the hip unit corresponding to different packet (or buffer) size. On the other hand, with the packet size increasing, the response of

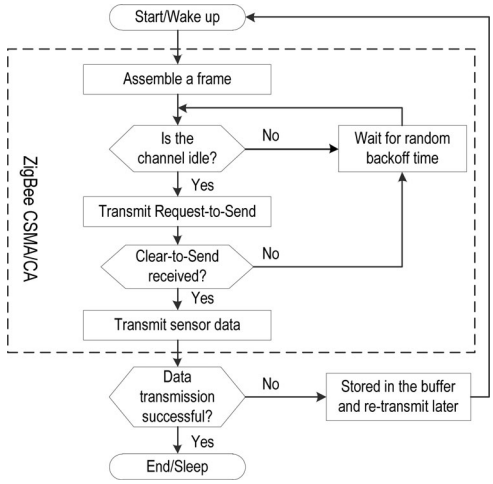

Fig. 8. Flowchart for anticollision and reliability control in WIMS.

the system will slow down, as seen in the increased real-time latency in Fig. 7. Selection of the packet size, therefore, needs to concurrently consider both energy efficiency and real-time latency: achieving energy efficiency requires large packet size, while satisfying real-time monitoring requires small packet size.

In the WIMS design, data packaging is based on the API mode of the ZigBee module, by which the sampling interrupt will disable data packaging and transmission if the data transmitting time exceeds the sampling period. For a 30-Hz sampling frequency, the maximum packet size (number of sensor packet being packetized) is limited to 16. As the packet size increases from 1 to 16, the supply current decreases, and reaches a minimum value when the packet size is 11. This is because the maximum payload of one ZigBee packet of the XBee module is 72 bytes (consisting of 2-bytes BOF + 2-bytes sensor ID + 66-bytes sensor data + 2-bytes EOF). If the packet size increases beyond 11, e.g., from 12 to 16, two packets will be needed to deliver the data. Accordingly, the supply current increases again. For the optimal packet size of 11, the corresponding latency is 366 ms, sufficient for real-time PA monitoring. The supply current at this packet size for the sensor, MCU and ZigBee module is 5.4 mA, which is about 50% less than that required by some of the commercially available wireless sensors [23].

2) Anticollision for transmission reliability. Data collision is one of the main problems in wireless communication system, which causes serious data loss and reduces communication speed [22]. Collision is also one of the major power wastages in wireless body sensor networks [15], [19]. For low-power data streaming, integrating the ZigBee-based communication protocol with the CSMA/CA algorithm [18] provides a platform for data collision avoidance. Fig. 8 shows a control flowchart of the WIMS protocol for data anticollision and reliable data transmission.

Before data transmission starts, an SN first listens to the channel for a predetermined amount of time to detect if another SN within the receiving range is occupying the channel. Upon detection of channel occupancy, the communication interval will be extended by a randomly truncated binary exponential back-off time [18]. To further enhance transmission reliability, each SN

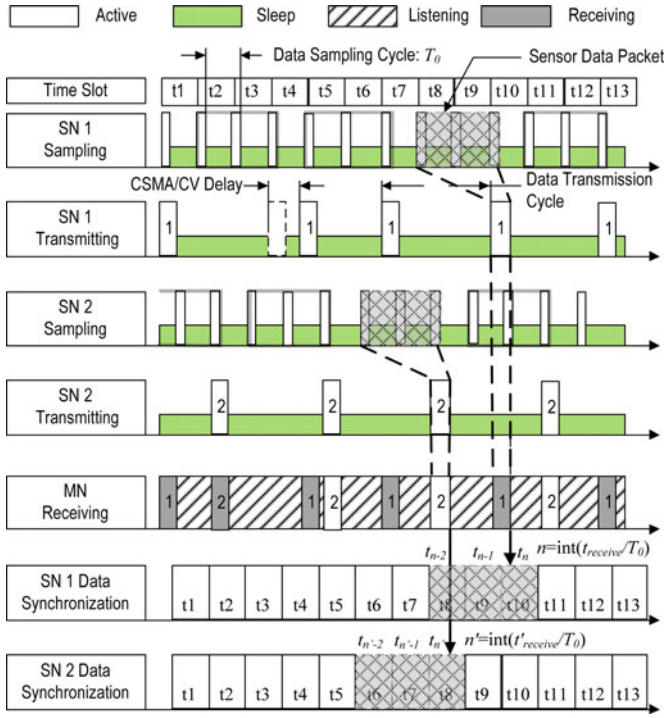

Fig. 9. WIMS data synchronization protocol (package no. = 3).

will probe the communication channel periodically and transmit data if the channel is free for at least two consecutive probing periods. After receiving the clear-to-send acknowledgment from the MN, an SN will initiate data transmission. A transmission status message Acknowledgment integrated in the ZigBee API frame will be sent back to the SN when the transmission is completed to indicate that the packet has been transmitted successfully. If the channel remains busy during the probing period, a transmission failure is acknowledged. The sensor data will then be stored in the buffer and be transmitted during the next cycle of transmission.

3) Data synchronization. Sensor data from different SNs received by the MN can be out of synchronization because of the packet size and system clock variations. As each SN packetizes its own data, the start and end times of the packetized data are not synchronized with those of other SNs. This problem becomes more evident as the packet size increases, because with more SNs joining the group, the deviation in the starting time of the data can quickly grow to equal the time of one transmission cycle of the packetized frame. Another factor that increases the time deviation is variations in the system clock. Consequently, the communication cycle of each SN can start at different times. As an example, if the clock in one SN has an accuracy of 20 parts per million (ppm), the maximum possible time deviation can reach 400 ms after a 10-h system uptime, without considering the effects of temperature-induced drift and transmitting cycle differences, both of which may further increase the deviation.

To minimize time deviation and maintain data synchronization, a slot-data-synchronization method has been devised, as shown in Fig. 9.

Sensor data in each packet received by the MN are allocated in the specific receiving buffer, based on the sensor ID stored in

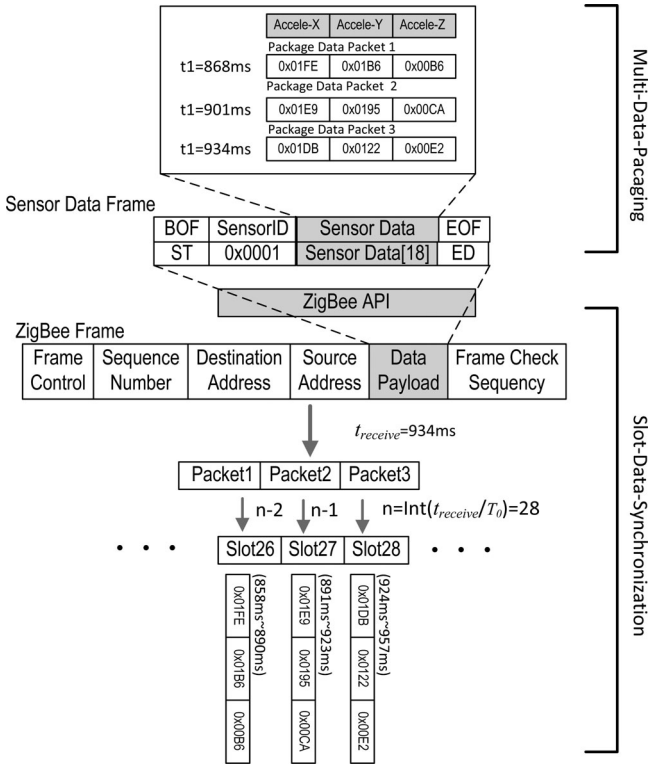

Fig. 10. Illustration of multidata packaging and slot-data-synchronization with real values of ZigBee API frame generated during transmission process. (Take the wrist unit as example, suppose package no. = 3.)

the sensor data frame. Each receiving buffer is tagged by a time index, and data are allocated into the correct time slot according to the packet receiving time. Consider a scenario where data from two SNs, SN1 and SN2, need to be synchronized. As shown in Fig. 9, the two SNs will wake up from *sleep*, and sample data at every T_0 time. The data are stored in the temporary buffer until it reaches the predetermined packet size based on the energy efficiency and real-time latency criterion. The SN will then packetize the data in the buffer and transmit to the MN. Assuming the time when the MN receives the packet is t_{receive}, the time index of the last sensor data frame n in the packet can be back calculated as

$$n = \text{Int}\left(\frac{t_{\text{receive}}}{T_0}\right) \tag{2}$$

where int is the floor function, which takes the largest integer that is less than the value. If the packet size is p, the time index of the sensor data frames will be $n-p+1, n-p+2, \ldots, n-1$, and n. The data will then be allocated to the time slots, t_{n-p+1} to t_n, and data synchronization among different SNs is achieved. In Fig. 10, multidata packaging and slot-data-synchronization with real values of ZigBee API frame generated during transmission process is illustrated.

IV. Experimental Evaluation

A. System Functionality

To test the functionality of the WIMS, data sampled from the four sensors were transmitted to a laptop computer via a ZigBee module (see Fig. 11). The data are displayed subsequently in real time, through a MATLAB program. The WIMS is worn by a human subject performing various types of activities, such as driving, walking, climbing stairs, life style activities, etc. In Fig. 12, sample signals from the hip and wrist accelerometers and the ventilation sensor are shown.

Fig. 11. Experimental setup for testing WIMS functionality.

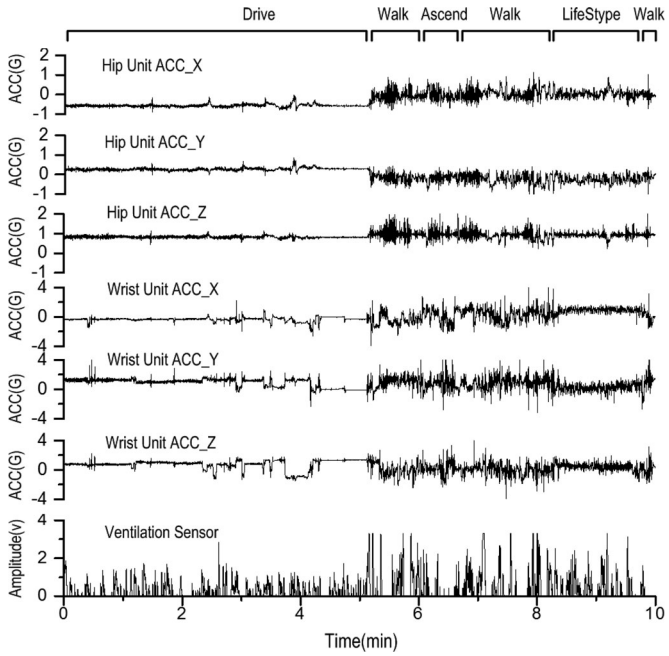

Fig. 12. Sample signals from the hip and wrist accelerometers and the ventilation sensor.

It is seen from the transmitted waveforms that: 1) the accelerometers are able to capture body motions along the different axial directions; 2) the ventilation sensor can capture the breathing frequency and volume. The results have demonstrated the functionality and wireless connectivity of the WIMS.

B. Communication Performance

Performance of real-time communication of the WIMS was experimentally evaluated, in terms of energy efficiency, communication reliability, and data synchronization of the SNs. Energy efficiency is reflected in the battery life, whereas quality of data synchronization is measured by the consistency of data transmission among different SNs. Performance of the algorithm is characterized by the time deviation of the data received in the MN from different SNs.

Time deviation between the x-axes of the accelerometer data in two SNs (hip unit and wrist unit) with three different

TABLE I
COMPARISON OF TIME DEVIATION FOR DIFFERENT ACTIVITIES

Physical Activity[a]	Testing No	Without Data Synchronization	With Data Synchronization
Walking	1	312.72s	22.52s
	2	348.72s	19.32s
	3	280.16s	47.04s
Running	1	176.68s	15.84s
	2	158.56s	16.24s
	3	155.38s	30.50s
Computer work	1	364.08s	4.68s
	2	389.27s	39.57s
	3	369.69s	18.96s
Average (Mean±SD)	----	283.92s	23.85s

[a] Only the x axis signals of the accelerometers of the Hip Unit and the Wrist Unit are compared. Time deviation of every second of the accelerometer signals from 0 to 30 seconds were recorded and analyzed. Final value is the mean value of these records.

TABLE II
PERFORMANCE SPECIFICATIONS OF COMPARISON RESULTS

Comparison Item	Battery Life [a]	Maximum Latency	Data Time Deviation
Without communication algorithms ($P = 1$)	16 hours	33.3 ms	33.3 ms
With communication algorithms ($P = 11$)	68 hours	366 ms	23.8 ms

[a] Battery life was based on a 370-mAh capacity. Data sampling rate is 30 Hz.

physical activities are shown in Table I, for the SN packet size of 11. For the two units, time deviation between the signals was calculated through cross correlation. It is seen that without data synchronization, the average time deviation between the signals is 283.92 ms, whereas with data synchronization, the time deviation is effectively reduced to 23.85 ms.

The performance of the WIMS with and without the two designed communication algorithms is compared in Table II. "Without communication algorithm" refers to no packaging and no data synchronization. In this mode, a packet is transmitted every 33.3 ms. "With communication algorithms" refers to transmission with the multidata packaging and slot-data-synchronization algorithms, for which a set of 11 packets are transmitted together. It is seen that, with algorithms, the energy efficiency and the data time deviation among different SNs are significantly improved (battery life increased from 16 to 68 h, and data time deviation from 33 ms down to 23.8 ms), and the maximum latency is within the required range (less than 400 ms). These results demonstrate good performance of the communication protocol in achieving low power consumption and reliable data synchronization.

C. Lab-Controlled PA Assessment

Experiments under laboratory controlled conditions have been conducted for evaluating the performance of WIMS on predicting the MET of human subject engaged in physical activities of various intensities. The MET is a measure for the intensity of aerobic exercise, and is calculated as the ratio of metabolic rate during a PA to the metabolic rate at rest. Three

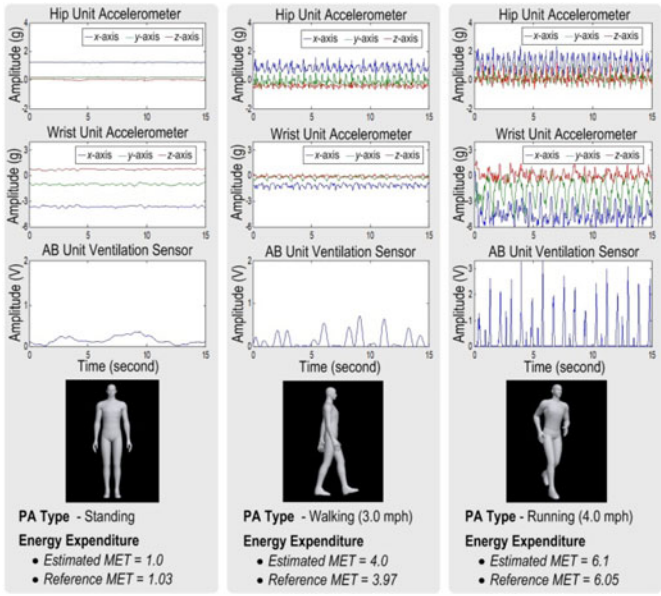

Fig. 13. PA assessment. (MET calculation described in [20].)

subjects were asked to perform three different types of activities for 7 min each, including standing, walking (on treadmill at 3.0 mph) and running (on treadmill at 4.0 mph). Data were collected by both the WIMS and a portable indirect calorimetry respiratory gas exchange system (Oxycon Mobile, Cardinal Health), which provides the reference measure of the energy expenditure. A multisensor data fusion algorithm [24] based on support vector machines (SVM) has been applied to the WIMS data to predict METs. Fig. 13 shows examples of sensors signals measured by the WIMS and the corresponding MET predictions under the three activities. These results have demonstrated the effectiveness of the WIMS in assessing PA energy expenditure.

D. Free-Living PA Assessment

To further evaluate the performance of the WIMS under free-living conditions, experiments were conducted on eight healthy subjects (three males, five females), with the following characteristics: (mean $\pm$ standard deviation): age $= 25.9 \pm 7.0$ years, mass $= 70.0 \pm 12.9$ kg, height $= 166.8 \pm 12.8$ cm, and body mass index $= 25.2 \pm 3.7$ kg/m^2. Each experiment consisted of a 2-h session where the subjects performed their day-to-day activities, e.g., computer work, driving to work, walking stairs, life style activities, etc. During the experimental session, the subject was directly observed by a trained researcher who recorded the activities on a hand-held palm device. The researcher stayed as inconspicuous as possible and did not interfere with the subject's activities by maintaining minimal contact with the subject.

Similar to the lab-controlled experiment, WIMS data for free-living experiments were segmented into 30-s nonoverlapping windows, which were then analyzed by the multisensor fusion algorithm developed in [20] to predict the intensity level of the free-living activities. As a preliminary analysis, the prediction was categorized into two levels: sedentary ($<$1.8 METs) and active ($\geq$1.8 METs). The results were compared with the

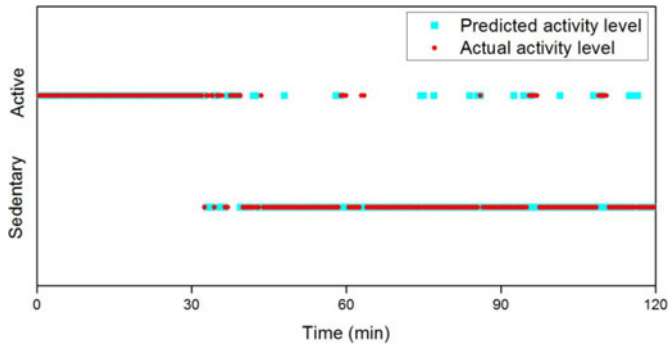

Fig. 14. Example of the actual and predicted activity levels from Subject 2.

TABLE III
PREDICTION OF ACTIVITY INTENSITY LEVEL

Subject No	Prediction Accuracy	Subject No	Prediction Accuracy
1	76.3%	5	94.4%
2	85.1%	6	92.5%
3	88.7%	7	94.2%
4	67.2%	8	89.9%
Overall accuracy		86.0%±9.6%	

researcher's direct observation which serves as the criterion measure. Fig. 14 shows an example (Subject 2) of the actual and predicted activity levels, and Table III shows the prediction accuracy for each subject. It is seen that the WIMS correctly recognized the activity intensity level 86% of the time, and these preliminary results have demonstrated the performance of the WIMS for PA assessment under free-living conditions.

V. CONCLUSION

In this paper, a ZigBee-based wireless wearable multisensor integrated measurement system (WIMS) for real-time PA monitoring and assessment is presented. Detailed analysis was performed for the WIMS hardware design and communication protocol. The WIMS communication protocol integrating the algorithms of multidata packaging and slot-data-synchronization has shown to have enhanced the energy efficiency and communication reliability. Specifically, the multidata packaging algorithm increases the battery life by about 325% (from 16 to 68 h) as compared to the system without the protocol. The slotdata-synchronization algorithm maintains data synchronization among the different SNs and reduces the data time deviation by 12 times (from 284 down to 24 ms). The effectiveness of the WIMS on assessing physical activities has been evaluated through experiments conducted under both lab-controlled and free-living conditions. Results have demonstrated good performance of the WIMS, in terms of functionality, communication, and energy efficiency. Future work will include the system improvement on compact design and *in situ* large-scale subject testing of the WIMS for PA assessment.

REFERENCES

[1] G. Fletcher, G. Balady, S. Blair, J. Blumenthal, C. Caspersen, B. Chaitman, S. Epstein, E. Froelicher, V. Froelicher, I. Pina, and M. Pollock, "Statement on exercise: Benefits and recommendations for physical activity programs for all americans," *Circulation*, vol. 94, pp. 857–862, 1996.

[2] V. Diaz, P. Benito, A. Peinado, M. Alvarez, C. Martin, V. Salvo, F. Pigozzi, N. Maffulli, and F. Calderon, "Validation of a new portable metabolic system during an incremental running test," *J. Sports Sci. Med.*, vol. 7, pp. 532–536, 2008.

[3] D. Hendelman, K. Miller, C. Baggett, E. Debold, and P. Freedson, "Validity of accelerometry for the assessment of moderate intensity physical activity in the field," *Med. Sci. Sports Exercise*, vol. 32, pp. 442–449, 2000.

[4] M. Mathie, A. Coster, N. Lovell, and B. Celler, "Accelerometry: Providing an integrated, practical method for long-term, ambulatory monitoring of human movement," *Physiol. Meas.*, vol. 25, pp. R1–R20, 2004.

[5] D. Pober, J. Staudenmayer, C. Raphael, and P. Freedson, "Development of novel techniques to classify physical activity mode using accelerometers," *Med. Sci. Sports Exercise*, vol. 38, pp. 1626–1634, 2006.

[6] K. D. Nguyen, I. M. Chen, Z. Q. Luo, S. H. Yeo, and H. B. L. Duh, "A wearable sensing system for tracking and monitoring of functional arm movement," *IEEE/ASME Trans. Mechatronics*, vol. 16, no. 2, pp. 213–220, Apr. 2011.

[7] A. U. Alahakone and S. Senanayake, "A real-time system with assistive feedback for postural control in rehabilitation," *IEEE/ASME Trans. Mechatronics*, vol. 15, no. 2, pp. 226–233, Apr. 2010.

[8] O. Aziz, L. Atallah, B. Lo, M. ElHelw, L. Wang, Z. G. Yang, and A. Darzi, "A pervasive body sensor network for measuring postoperative recovery at home," *Surg. Innov.*, vol. 14, pp. 83–90, Jun. 2007.

[9] P. Bonato, "Wearable sensors and systems," *IEEE Eng. Med. Biol. Mag.*, vol. 29, no. 3, pp. 25–36, May 2010.

[10] E. Monton, J. F. Hernandez, J. M. Blasco, T. Herve, J. Herve, J. Micallef, I. Grech, A. Brincat, and V. Traver, "Body area network for wireless patient monitoring," *IET Commun.*, vol. 2, pp. 215–222, Feb. 2008.

[11] V. Leonov, T. Torfs, P. Fiorini, and C. Van Hoof, "Thermoelectric converters of human warmth for self-powered wireless sensor nodes," *IEEE Sens. J.*, vol. 7, no. 5, pp. 650–657, May/Jun. 2007.

[12] B. S. Lin, N. K. Chou, F. C. Chong, and S. J. Chen, "RTWPMS: A real-time wireless physiological monitoring system," *IEEE Trans. Inf. Technol. Biomed.*, vol. 10, no. 4, pp. 647–656, Oct. 2006.

[13] A. Milenkovic, C. Otto, and E. Jovanov, "Wireless sensor networks for personal health monitoring: Issues and an implementation," *Comput. Commun.*, vol. 29, pp. 2521–2533, Aug. 2006.

[14] J. C. Yao, R. Schmitz, and S. Warren, "A wearable point-of-care system for home use that incorporates plug-and-play and wireless standards," *IEEE Trans. Inf. Technol. Biomed.*, vol. 9, no. 3, pp. 363–371, Sep. 2005.

[15] S. J. Marinkovic, E. M. Popovici, C. Spagnol, S. Faul, and W. P. Marnane, "Energy-efficient low duty cycle MAC protocol for wireless body area networks," *IEEE Trans. Inf. Technol. Biomed.*, vol. 13, no. 6, pp. 915–925, Nov. 2009.

[16] E. Jovanov, A. Milenkovic, C. Otto, and P. C. De Groen, "A wireless body area network of intelligent motion sensors for computer-assisted physical rehabilitation," *J. Neuroeng. Rehabil.*, vol. 2, p. 6, Mar. 1, 2005.

[17] M. F. Rasid and B. Woodward, "Bluetooth telemedicine processor for multichannel biomedical signal transmission via mobile cellular networks," *IEEE Trans. Inf. Technol. Biomed.*, vol. 9, no. 1, pp. 35–43, Mar. 2005.

[18] J. S. Lee, "Performance evaluation of IEEE 802.15.4 for low-rate wireless personal area networks," *IEEE Trans. Consum. Electron.*, vol. 52, no. 3, pp. 742–749, Aug. 2006.

[19] O. Omeni, A. C. W. Wong, A. J. Burdett, and C. Toumazou, "Energy efficient medium access protocol for wireless medical body area sensor networks," *IEEE Trans. Biomed. Circuits Syst.*, vol. 2, no. 4, pp. 251–259, Dec. 2008.

[20] S. Liu, R. Gao, D. John, J. Staudenmayer, and P. Freedson, "Multi-sensor data fusion for physical activity assessment," *IEEE Trans. Biomed. Eng.*, vol. 59, no. 3, pp. 687–696, Mar. 2012.

[21] S. Liu, R. Gao, and P. Freedson, "Design of a wearable multi-sensor system for physical activity assessment," in *Proc. IEEE/ASME Int. Conf. Adv. Intell. Mechatronics*, Jul. 2010, pp. 254–259.

[22] Q. Sun, H. Zhang, and L. Mo, "Dual-reader wireless protocols for dense active RFID identification," *Int. J. Commun. Syst.*, vol. 24, Mar. 2011.

[23] A. Burns, B. R. Greene, M. J. McGrath, T. J. O'Shea, B. Kuris, S. M. Ayer, F. Stroiescu, and V. Cionca, "SHIMMER (TM): A wireless sensor platform for noninvasive biomedical research," *IEEE Sens. J.*, vol. 10, no. 9, pp. 1527–1534, Sep. 2010.

[24] S. Liu, R. X. Gao, D. John, J. Staudenmayer, and P. Freedson, "SVM-based multi-sensor fusion for free-living physical activity assessment," in *Proc. IEEE 33rd Annu. Int. Conf. Eng. Med. Biol. Soc.*, Boston, MA, Aug./Sep. 2011, pp. 3188–3191.